Angular Momentum properties of structures with N-body simulations

E. D'Onghia, G.Lufkin,J.Pizagno
Advisor: T. Quinn

July 15, 1998

Aim of this project is to investigate the behavior of angular momentum of structures (cluster of galaxies, halos in a cluster and particles in halos) using N-body simulations. We study the growth of angular momentum with radius and the distribution of angular momentum in individual objects. Are explained physical concepts to understand this behavior.

1 Introduction

There are several reasons for angular momentum behavior of bound objects to be investigated with particular attention:

- To understand how exactly protogalactic systems acquired their angular momentum. Although efforts,it is not clear what mechanisms were responsable for the distribution of angular momentum in the luminous parts of galaxies. Before protogalaxies began to collapse several processes could have imparted angular momentum to them. Tidal mechanism was considered by Peebles (1969). He thought that if galaxies and clusters formed by gravitational instability of small density perturbations, they will have acquired angular momentum through tidal interactions with their neighbors. Analytic descriptions of this process are inadequate in modeling the non linear phase of structure formation. Peebles used linear theory to estimate the angular momentum growth in randomly placed spherical regions, assuming $P(k) \propto k^n$. He matched the results with those of a simple non linear model in which the torque on a protosystem was calculated as the product of its quadrupole moment with the tidal field of neighboring point masses.
  Although Peebles's calculation suggested that the dimensionless spin parameter: $\lambda = \frac{J\sqrt{E}}{GM^{5/2}} = 0.08$, detailed predictions from the tidal torquing model require N-body simulations.

- **Secondary Infall Paradigm**.
QSZ (Quinn,P. et al., 1988) showed that the final mass distribution in halos were linked to the properties of the initial $P(k)$ of density fluctuations in a manner implied by a secondary infall paradigm. In this paradigm the collapse of an object is idealized as the collapse of a system of spherical concentric shells. Each shell collapses preserving its total energy. For spherically symmetric perturbations this paradigm predicts the observed mass distribution of halos formed in cosmological N-body simulations.

- **Mestel hypothesis**.
Mestel proposed that the distribution of matter in a collapsed object could be determined from the initial distribution of angular momentum within a protogalaxy if each element of the protogalaxy conserved its specific angular momentum as it collapsed.

The N-body simulation that we analyzed is obtained using a nesting scheme to achieve higher spatial and mass resolution within a region of greatest interest from a "fair" volume of $100Mpc^3$ in a standard CDM Universe (Ghigna et. al, 1998). Particle distribution is evolved with a new high performance parallel treecode "PKDGRAV". Softening lenght is 5 Kpc, the final virial radius of the cluster is 2 Mpc and the mass is 4.6 $10^{14}M_\odot$ (Moore et al., 1997).

2 Alignment in inner cluster halo

We computed the alignment of angular momentum of particles within the inner halo (central group) of the cluster. The halo was divided up into a number of shells in radius. For each shell, a cumulative alignment parameter Γ was defined as:

$$\Gamma(r) = \frac{J(r' < r)J_{tot}}{|J(r' < r||J_{tot}|} \tag{1}$$

with $J(r' < r)$ total vector angular momentum of all particles with radius less then r, and J_{tot} the total vector angular momentum of the halo.
We expected that in a halo well-mixed (without substructures), all parts are alligned. In other words we expect that the mean angular momentum content with radius is the same as this for the same mass distribution in which all orbits of the particles are aligned and circular. This behavior is expected if mixing and momentum transport during the relaxation of the halo are efficient in aligning the mean angular momentum of matter at different radius.

Fig.1 (top) shows no alignment. There are three possible reasons why there is no alignment:

- The choise of binning in radius is not correct. Infact if binning is too much short we probably sample noise.

- A difficult in gravitational clustering is that there are no well- defined boundaries which delineate the virialized regions from the outer parts of halos or of cluster. Bound objects are identified with FOF scheme, so we don't exactly know if we take in account all particles of the halo. This "bias" affect the definition of total angular momentum of particles. For this reason we show in Fig.1 (bottom) the cumulative alignment parameter computed in shells in radius outer the size of inner group. This figure shows that there is alignment.
- The presence of substructures and unvirialized systems can produce no alignment (Barnes and Efstathiou, 1987).

Fig.2 shows the alignment parameter for other individual halos selected. There is no alignment for the same reasons described above.

3 Alignment of halos in cluster

We computed the alignment parameter Γ of total angular momentum of all halos related to the angular momentum of the center of the cluster. The cluster was divided up into a number of shells in binning radius. Inner halos are less bound then outer. A trend to alignment is showed in Fig.3 (top panel).

4 The radial distribution of Angular momentum in inner halo

For inner halo we computed the cumulative radial distribution of angular momentum:

$$J(r) = \sum_{i=1}^{N} |J_i(r' < r)| \tag{2}$$

where the subscripts refer to sums of the individual particle angular momenta. We expect that tidal torquing from neighboring systems introduces a linear growth in the angular momentum content of a given shell. Inner shells turn around and collapse sooner than outer shells. There is a gradient in angular moment. The angular moment is transported from the inner parts of groups to their outer parts by gravitational torques. The angular momentum for matter near the center of a group is lower than that for matter in the outer parts. So we expect $J(r) \propto r$. This behavior is found when we consider shells in radius outer the size of inner group (Fig.4 (bottom panel)) Fig.4 (top panel) shows the distribution of $J(r)$ for the central inner halo if the binning in radius is within the size of central group. The same trend is showed in Fig.3 (bottom panel) for cumulative radial distribution of angular momentum of halos in cluster.

5 Conclusions

We find a trend towards alignment of angular momenta when we compute the total angular momentum of all halos related to the angular momentum of the center of the cluster. However, regarding individual halos we can't find any alignment for the inner group mainly for three reasons: the possible presence of substructures in a halo, a not correct binning in radius and not well- defined boundaries to delineate the virialized regions from the outers. Furthermore we think that Mestel hypothesis is incorrect when applied to formation of dissipationless structure by dynamical friction. Although the global specific angular momentum of each individual halos may be conserved (if we consider an isolated halo), the distribution of specific angular momentum in the halo is rearranged by the collapse. Infact we expect the tidal torque from neighboring systems to introduce a linear growth in the angular momentum content of a given shell. Inner shells turn around and collapse sooner than outer shells, thus producing a gradient of J into the protohalo. In future we suggest different choises of binning in radius. An idea could be to compute in each shell of the halo the same number of particles. An other idea could be to estimate the isotropy of individual particle orbits and the eccentricity of each orbit as a function of binding energy.

References

Barnes and Efstathiou, 1987, Ap.J, 319: 576-600
Quinn,P. and Zurek, 1988, Ap.J, 331: 1-18
Ghigna,S.,Moore,B.,Governato,F., 1998, M.N.R.A.S, 0,1-7

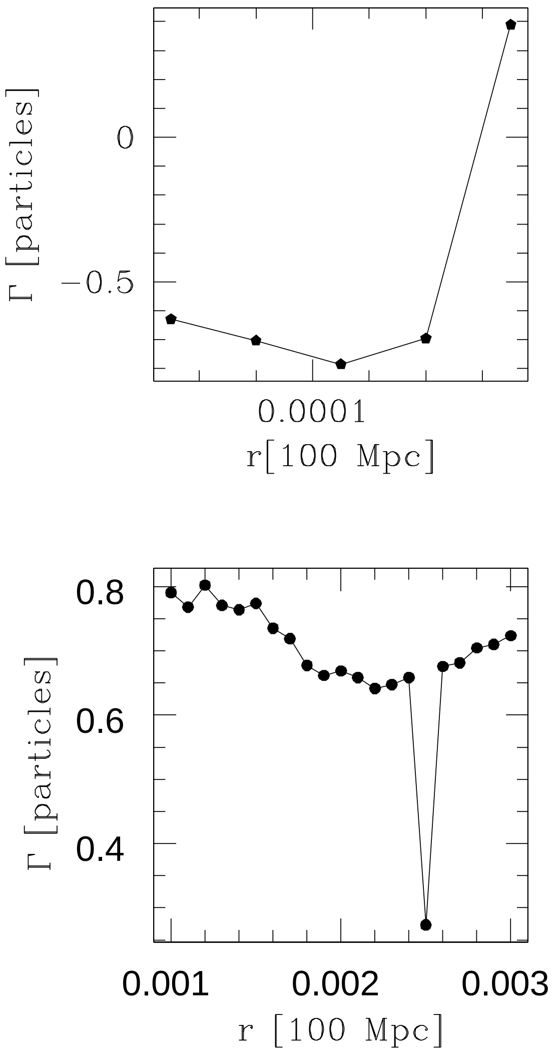

$$\Gamma = \frac{J(r' < r) J_{tot}}{|J(r' < r)||J_{tot}|}$$

Figure 1:

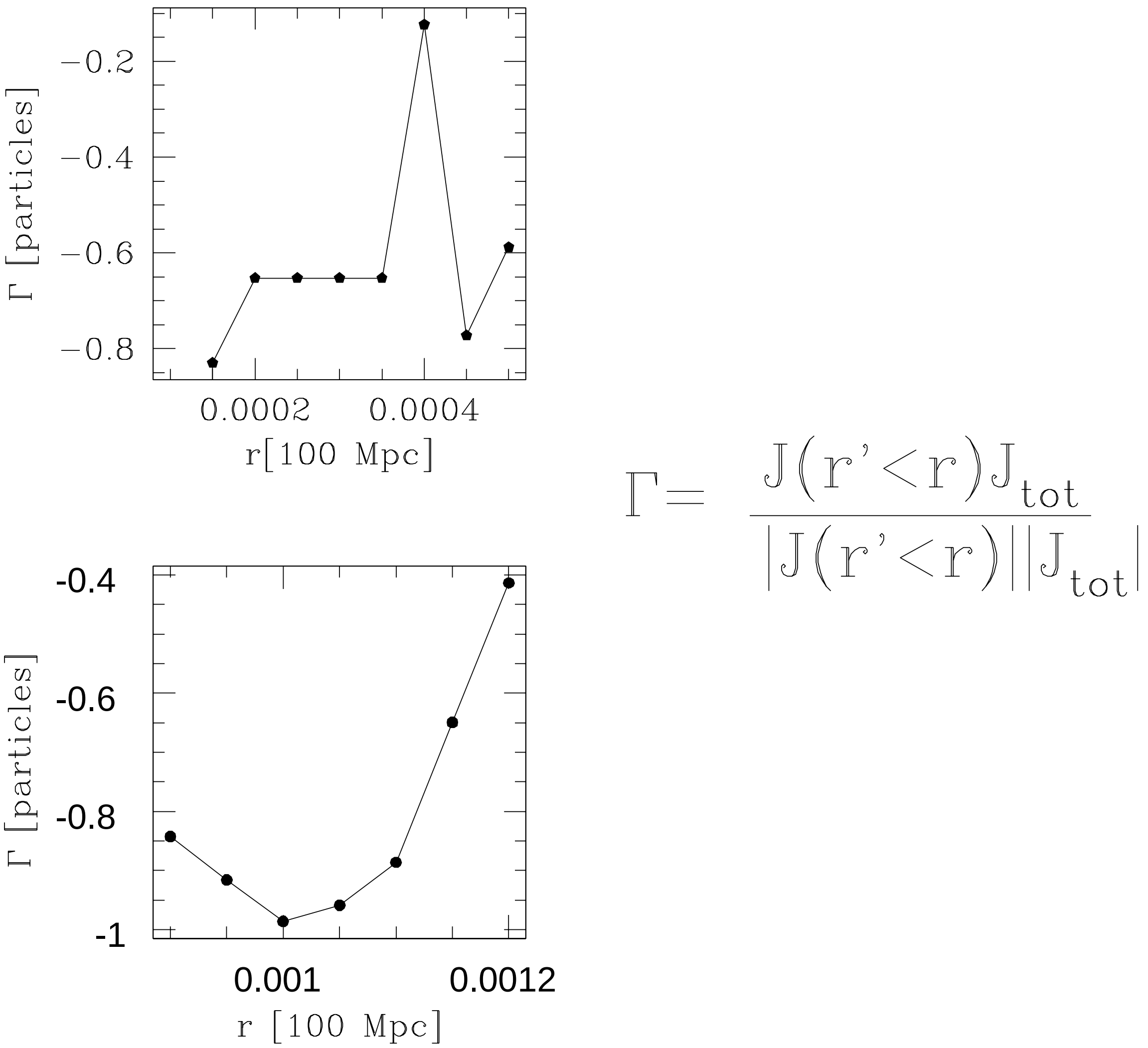

−0.2
−0.4
−0.6
−0.8
Γ [particles]
0.0002
0.0004
r[100 Mpc]
$\Gamma = \frac{J(r'<r) J_{tot}}{|J(r'<r)||J_{tot}|}$
-0.4
-0.6
-0.8
-1
Γ [particles]
0.001
0.0012
r [100 Mpc]

Figure 2:

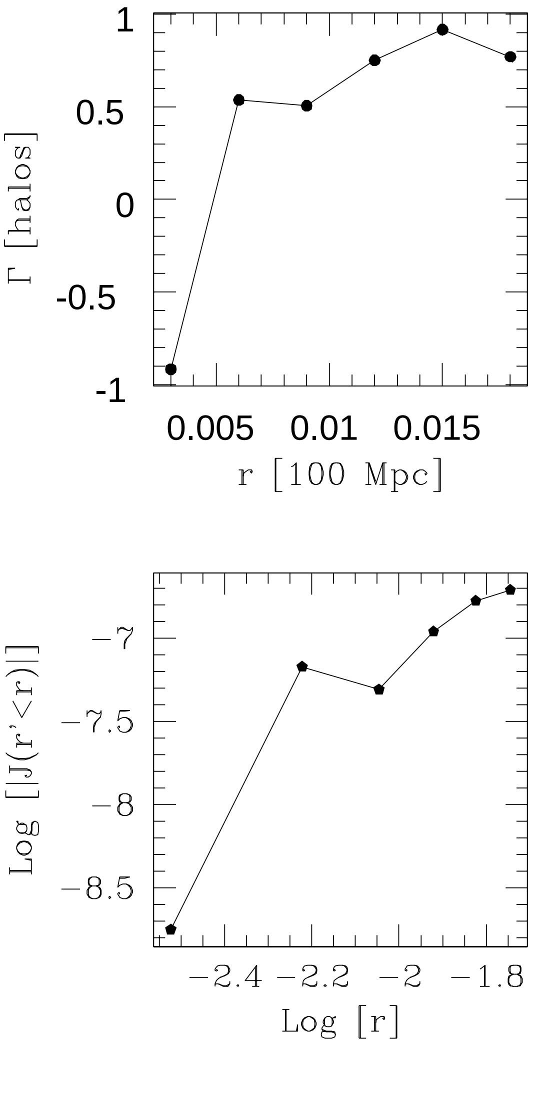

1
0.5
0
-0.5
-1
Γ [halos]
0.005
0.01
0.015
r [100 Mpc]
−7
−7.5
−8
−8.5
Log [|J(r'<r)|]
−2.4
−2.2
−2
−1.8
Log [r]

Figure 3:

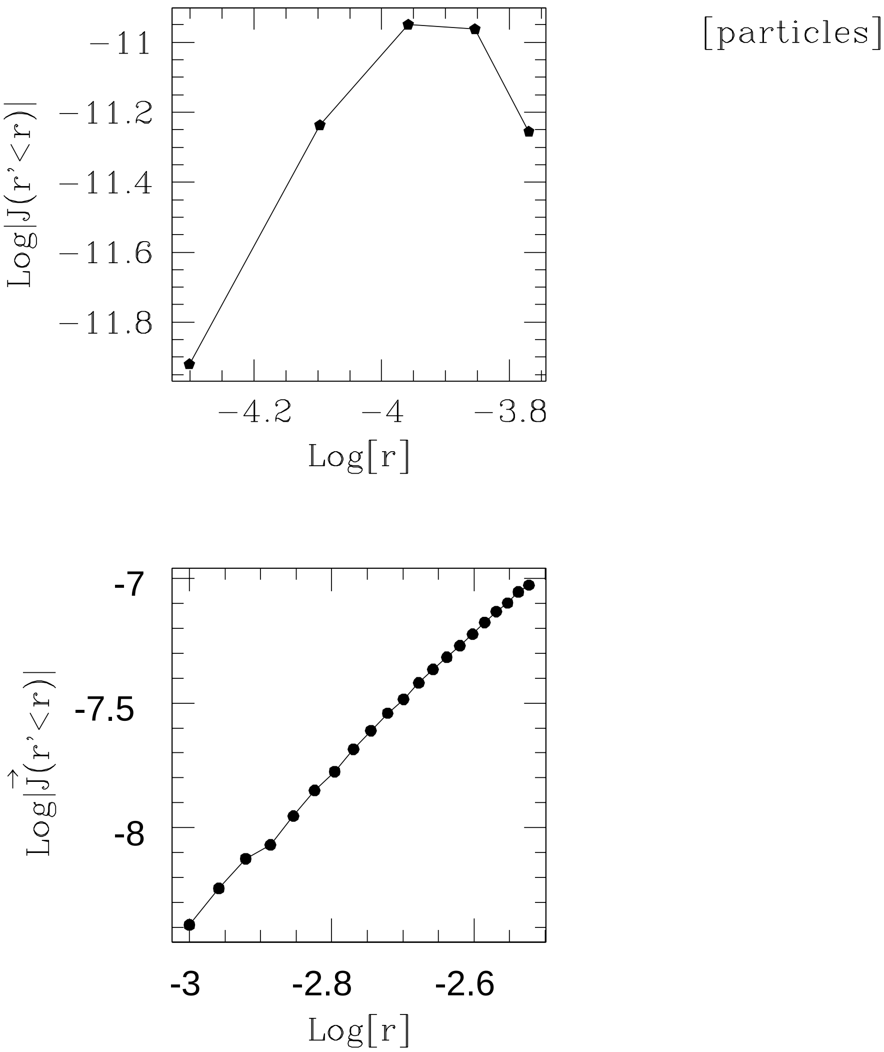
[particles]
−11
−11.2
−11.4
−11.6
−11.8
$\mathrm{Log}|\vec{J}(r'<r)|$
−4.2
−4
−3.8
Log[r]
-7
-7.5
-8
$\mathrm{Log}|\vec{J}(r'<r)|$
-3
-2.8
-2.6
Log[r]

Figure 4: